ISPRS Journal of Photogrammetry and Remote Sensing 188 (2022) 190–200

Contents lists available at ScienceDirect

ISPRS Journal of Photogrammetry and Remote Sensing

journal homepage: www.elsevier.com/locate/isprsjprs

Deep transfer learning of global spectra for local soil carbon monitoring

Zefang Shen [a], Leonardo Ramirez-Lopez [b], Thorsten Behrens [c,d], Lei Cui [e], Mingxi Zhang [a], Lewis Walden [a], Johanna Wetterlind [f], Zhou Shi [g], Kenneth A Sudduth [h], Philipp Baumann [d], Yongze Song [i], Kevin Catambay [a,e], Raphael A. Viscarra Rossel [a,*]

[a] Soil and Landscape Science, School of Molecular and Life Sciences, Curtin University, GPO Box U1987, Perth, WA 6845, Australia
[b] Data Science Department, BUCHI Labortechnik AG, Flawil 9230, Switzerland
[c] Soil and Spatial Data Science, Soilution GbR, Heiligegeiststrasse 13, 06484 Quedlinburg, Germany
[d] Compentence Center for Soils (KOBO), School of Agricultural, Forest and Food Sciences (HAFL), Bern University of Applied Sciences, Länggasse 85, 3052 Zollikofen, Switzerland
[e] Department of Mechanical Engineering, Curtin University, GPO Box U1987, Perth, WA 6845, Australia
[f] Department of Soil and Environment, Swedish University of Agricultural Science, PO Box 234, SE-532 23 Skara, Sweden
[g] Institute of Agricultural Remote Sensing and Information Technology Application, College of Environmental and Resource Sciences, Zhejiang University, Hangzhou 310058, China
[h] USDA-ARS Cropping Systems & Water Quality Research Unit, Columbia, MO 65211, USA
[i] School of Design and the Built Environment, Curtin University, GPO Box U1987, Perth, WA 6845, Australia

ARTICLE INFO

Keywords:
Soil organic carbon
Visible–near-infrared spectra
Transfer learning
Deep learning
Spectral library

ABSTRACT

There is global interest in spectroscopy and the development of large and diverse soil spectral libraries (SSL) to model soil organic carbon (SOC) and monitor, report, and verify (MRV) its changes. The reason is that increasing SOC can improve food production and mitigate climate change. However, 'global' modelling of SOC with such diverse and hyperdimensional SSLs do not generalise well locally, e.g. at a field scale. To address this challenge, we propose deep transfer learning (DTL) to leverage useful information from large-scale SSLs to assist local modelling. We used one global, three country-specific SSLs and data from three local sites with DTL to improve the modelling and localise the SOC estimates in individual fields or farms in each country. With DTL, we transferred instances from the SSLs, representations from one-dimensional convolutional neural networks (1D-CNNs) trained on the SSLs, and both instances and representations to improve local modelling. Transferring instances effectively used information from the global SSL to most accurately estimate SOC in each site, reducing the root mean square error (RMSE) by 25.8% on average compared with local modelling. Our results highlight the effectiveness of DTL and the value of diverse, global SSLs for accurate local SOC predictions. Applying DTL with a global SSL one could estimate SOC anywhere in the world more accurately, rapidly, and cost-effectively, enabling MRV protocols to monitor SOC changes.

1. Introduction

Soil stores more carbon (C) than all terrestrial vegetation and the atmosphere combined (Schlesinger, 1977; Field and Raupach, 2004). Soil organic carbon (SOC) is central to human welfare. It can improve ecosystems health, biodiversity, and food security (Lal, 2004) by helping to retain and release nutrients in the soil and to develop structure and soil biodiversity (Lehmann and Kleber, 2015). Soil can be a source or a sink of C; it can be emitted to the atmosphere as carbon dioxide, accelerating climate change, but also, depending on the environment and management, it can trap C from the atmosphere to help mitigate climate change. Accurate and cost-effective measurements of SOC are needed for the measurement, monitoring, reporting and verification (MRV) of its status and to provide information on the response to land management interventions and policy design.

Visible–near-infrared (vis–NIR) spectroscopy is a rapid, non-destructive, non-polluting, and cost-efficient method for characterising soil properties such as SOC (Stenberg et al., 2010). Numerous efforts have been made in previous decades to develop soil spectral libraries (SSLs) over large areas and with diverse soil samples: at national

* Corresponding author.
E-mail address: r.viscarra-rossel@curtin.edu.au (R.A. Viscarra Rossel).

https://doi.org/10.1016/j.isprsjprs.2022.04.009
Received 16 November 2021; Received in revised form 3 April 2022; Accepted 14 April 2022
Available online 26 April 2022

(Viscarra Rossel and Webster, 2012; Shi et al., 2015; Wijewardane et al., 2016; Gogé et al., 2012; Dematte et al., 2019; Peng et al., 2013), continental (Orgiazzi et al., 2018), and global scales (Viscarra Rossel et al., 2016). The SSLs consist of soil properties (response variables or targets), corresponding spectra and metadata. Together, they are used to develop models to estimate the properties of soil samples using only their spectra. The spectroscopic measurements, modelling and estimation are relatively rapid and inexpensive. Thus, such libraries can help to supplement, reduce or, in some cases (e.g. measures of mineralogy), negate the need for conventional soil analysis with laboratory methods that are more time consuming and expensive(Liu et al., 2018). However, spectroscopic modelling using large SSLs is challenging (Gogé et al., 2014; Guerrero et al., 2014; Clairotte et al., 2016). The models developed tend to generalise poorly at a local scale (e.g. fields, farms or smaller regions), even when the local sites are within the library's scope (Wetterlind and Stenberg, 2010). Despite the significant and continuous investment to create large SSLs that represent soil variation at different scales, the poor generalisation of spectroscopic models developed with large SSLs diminishes their value for solving 'real-world' problems and therefore hinders the practical application of vis–NIR soil spectroscopy.

Large SSLs contain valuable information for local SOC modelling. They can help to reduce the need for expensive soil analysis for SOC monitoring at farms or fields. But how to effectively extract such information from the SSLs to accurately estimate SOC (and other soil properties) locally? Developing robust methods to leverage the useful information in large SSLs is important. This challenge has been the focus of research over the past decades (Naes et al., 1990; Shenk et al., 1997; Ramirez-Lopez et al., 2013). Several researchers have proposed methods to localise the modelling with SSLs, but with limited success, because their performance with different data, in various applications, and when the localisation is from a large (e.g. global) to a small (e.g. an agricultural field) level, is generally inconsistent (Seidel et al., 2019; Li et al., 2021; Tsakiridis et al., 2021). Spiking augments a SSL with a few labelled local data to form an augmented SSL for the modelling (Wetterlind and Stenberg, 2010; Brown, 2007; Sankey et al., 2008; Viscarra Rossel et al., 2009). It can also be implemented by making multiple copies of the local data to increase the weight of local data in the augmented SSL and thus their leverage in the modelling. The method is called spiking by extra-weighting (Guerrero et al., 2014, 2016). Methods based on spiking are easy to implement but they are very sensitive to the size of the SSL, the local data and there is no clear indication of the 'extra-weights' required, leading to their inconsistent performance (Gogé et al., 2014). Other methods subset a SSL based on spectral similarity using memory-based learning which selects neighbours of the local spectra in a SSL using distance metrics (Ramirez-Lopez et al., 2013; Shenk et al., 1997) or additionally constraining the SSL with geographical information (Shi et al., 2015). Spectroscopic models are then developed using the SSL subsets. Because these methods rely on spectral similarity, they only perform well when the SSLs hold spectra that are very similar, in terms of their information content, but also of their 'noise' characteristics, to the local data. Viscarra Rossel and Webster (2012) used regression trees to localise models by partitioning the entire SSL into 'branches' using conditions and then fitting local linear models at each 'leaf' separately. However, localising to a specific local farm/field can be difficult since the 'leaves' may not relate to the local site.

Transfer learning is a set of methods for localising models. It leverages information from a source problem with large volumes of data to assist a target problem with limited data because they are difficult or expensive to obtain. Transfer learning has successful applications in different domains (Mateo-García et al., 2020; Wurm et al., 2019; Gao and Cui, 2020; Guo et al., 2019; Cui et al., 2018; Zoph et al., 2016; Kang et al., 2021). It might also provide a solution for localising spectroscopic models by transferring whatever-related information is in the more extensive and diverse SSL to the estimation of the soil properties at the local site. There are different categorisations of transfer learning (Pan and Yang, 2009; Tan et al., 2018; Weiss et al., 2016), but generally, it can be categorised as instance-, representation-, parameter-, and relational-based transfer learning (Pan and Yang, 2009). There has been little exploration of these approaches in soil spectroscopy or soil science, more generally. Lobsey et al. (2017) developed a method that presents a form of instance-based transfer learning for localising spectroscopic models. This method, RS-LOCAL, performs a data-driven search by resampling an SSL, and recursively calibrates the response to the spectra in each subset using partial least squares regression (PLSR). The algorithm then retains only the most relevant data from the SSL for the modelling. Lobsey et al. (2017) compared RS-LOCAL to all other methods for localising the modelling (described above) and showed that it outperformed them.

Most recently, studies have reported on the transfer learning of representations (or learned features) using convolutional neural networks (CNNs), as a possible solution for localising spectroscopic models (Liu et al., 2018; Padarian et al., 2019). The transfer is performed by training a CNN on the more extensive SSL, then fixing the front layers and re-training the remaining ones on the local data. The representations learnt in the front layers are then transferred for the localised modelling with a CNN for the localised estimation. These studies report on the transfer of spectral information from a continental SSL (Orgiazzi et al., 2018) to the country level (Padarian et al., 2019), or more local situations (Liu et al., 2018), and only somewhat better results than other machine learning and statistical models. We found no research on the transfer learning of global or country SSLs for localising spectroscopic estimates of SOC at the farm- or field-scale.

A large SSL that captures soil variation globally is rich in information, but is also complex. If we could develop robust methods for transfer learning, large SSLs might enable rapid, cost-effective and accurate local estimates of SOC. The challenge is to develop such methods. Here, we hypothesise that for the spectroscopic modelling with deep learning, transferring instances and representations will more effectively improve the localisation and estimation of SOC than transferring only representations. Thus, our aims are to (i) transfer information from large SSLs with different complexity to localise the estimates of SOC. We used one global SSL and SSLs from three different countries, (ii) investigate three types of deep transfer learning (DTL) to transfer instances, transfer representations, and transfer both instances and representations, (iii) compare the DTL to estimates derived with models that use the entire SSLs and models that use only local data from each field or farm. To our best knowledge, there is no published research on the use of DTL that considers the transfer of instances or instances and representations.

2. Methods

2.1. Data

For our experiments, we used a recently compiled global SSL, the SSLs from three countries: China, Sweden, and the USA, and local data from a field or farm in each country. The global SSL encompasses a subset of the global spectral database described by Viscarra Rossel et al. (2016), the World Soil Information (ISRIC) spectral library (ICRAF, 2021; Shepherd et al., 2003), the European LUCAS database (Stevens et al., 2013), the Mediterranean spectral database (i-BEC, et al. 2019), and the Chinese spectral library described by Shi et al. (2014). The country SSLs were extracted from the global SSL and the local data were independent of the global and country SSLs. Locations of the global SSL and the local samples from each country are shown in Fig. 1a and their spectra in Fig. 1b. Relevant information on the data are summarised in Table 1. The number of samples in the global and country SSLs (K) range from 50,422 for the global to 2,319 for Sweden. Soil organic carbon (SOC) contents vary widely in the SSLs from 0.04% to 35.04%, whereas the SOC range in the local datasets is smaller, from 0.78% to 4.54%. The spatial extents of the local data range from 0.1 km^2 to 164.7 km^2.

From each of the local sites with N samples, we selected a subset of n

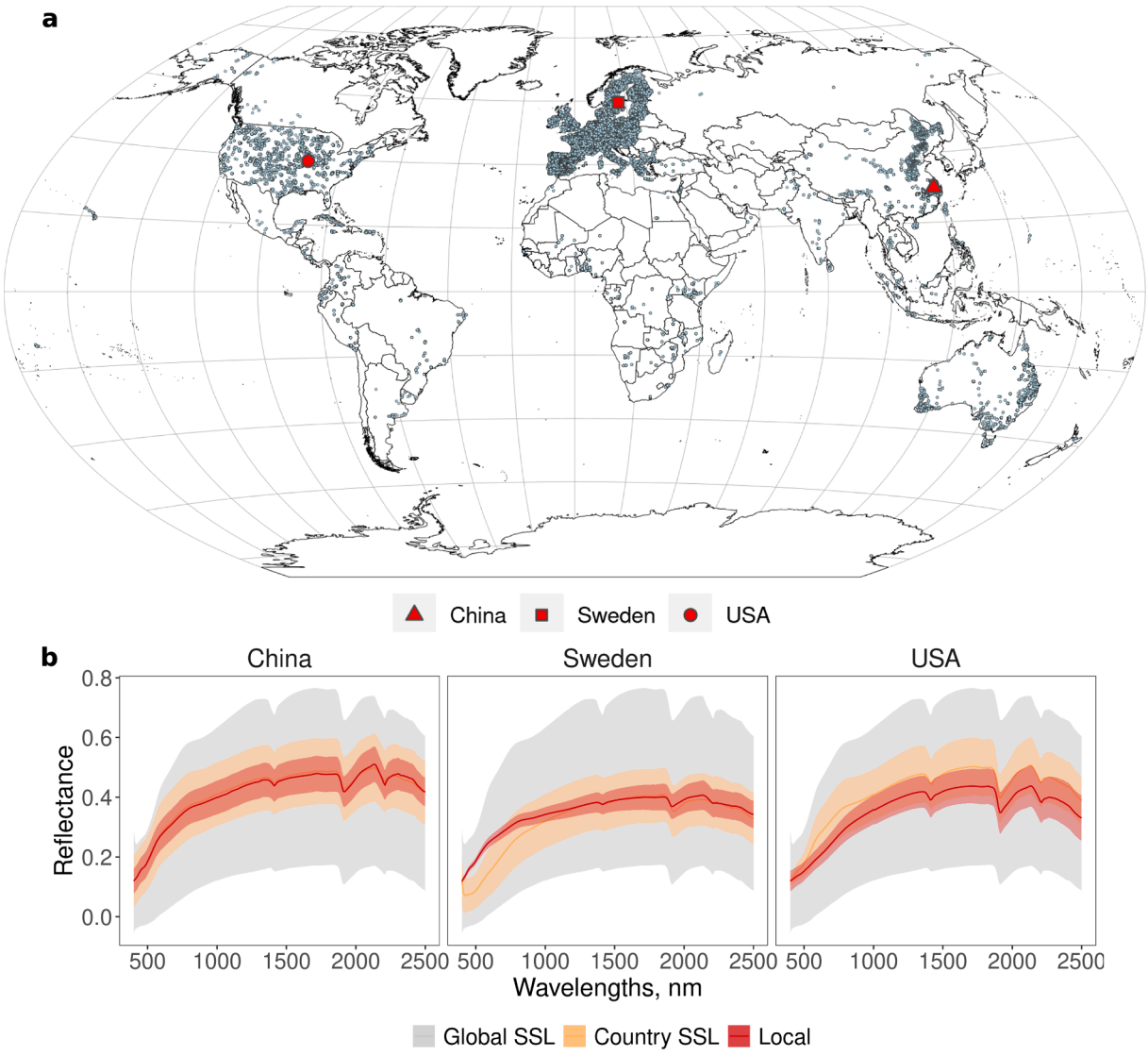

Fig. 1. (a) Location of data in the global spectral library (blue discs) and location of the local sites in China, Sweden, and the USA (red shapes). (b) Visible–near infrared reflectance spectra of the global SSL, the country SSLs, and local data.

Table 1
Information and statistical summaries of the data from the global and countries SSLs and the local data, showing the number of data in the global and country SSLs (*K*), the local sites (*N*), the area of the local sites, the soil types (A = Acrisols, B = Cambisols, W = Planosols) (Food and Agriculture Organisation, 1998), and the descriptive statistics of the SOC content. S.d. is the standard deviation, Q1 and Q3 are the first and third quartiles, Min. is the minimum and Max. the maximum of the SOC distribution.

				SOC (%)						
SSL	***K***			**Mean**	**S.d.**	**Min.**	**Q1**	**Median**	**Q3**	**Max.**
Global	50,422			2.28	3.56	0.04	0.55	1.26	2.50	35.04
China	5,183			1.61	1.85	0.04	0.78	1.27	1.94	31.40
Sweden	2,319			6.14	6.99	0.08	2.08	3.56	6.49	35.04
USA	4,155			1.20	1.98	0.04	0.22	0.52	1.30	24.16
Local data	***N***	**Area, km^2**	**Soil type**	**Mean**	**S.d.**	**Min.**	**Q1**	**Median**	**Q3**	**Max.**
China	135	164.7	A	1.74	0.58	0.89	1.41	1.59	2.05	4.54
Sweden	108	0.8	B, W	2.25	0.57	1.31	1.78	2.23	2.63	4.47
USA	216	0.1	W	1.62	0.63	0.78	1.10	1.43	2.05	3.74

= 30 representative samples for the modelling described below. The selection was performed with the Kennard-Stone algorithm (Kennard and Stone, 1969; Stevens and Ramirez-Lopez, 2014) using only the spectra. The remaining $N-n$ samples were unseen during the model development and used as the test set to validate the final models.

2.2. Spectral preprocessing

The measurements of the soil spectra, including spectrometers and protocols used for the measurements are described in Viscarra Rossel et al. (2016). The vis–NIR spectra in the library range from 400 nm to

2500 nm and have a wavelength spacing of 10 nm. In our experiments, we first converted the reflectance (R) spectra to apparent absorbance using $log_{10}(1/R)$ and applied the standard normal variate transform (SNV) to reduce multiplicative effects of scattering and particle size, and also to reduce differences in the intensities of the signals (Barnes et al., 1989). Other preprocessing methods were tested but not considered since preprocessing had little effect on the performance of optimised 1D-CNNs (Shen and Viscarra Rossel, 2021).

We performed a principal component analysis (PCA) (Wold et al., 1987) on the spectra from the global SSL, the country SSLs, the SSL localised and the local data, to visualise their relationships. PCA was first carried out on the global SSL and the other spectra were projected onto its principal component (PC) space. The first three PCs were plotted and used for interpretation.

2.3. Machine learning

2.3.1. Benchmark models

Fig. 2 shows the study design and experiments conducted. First, we developed optimised 1D-CNNs using the global or country SSLs and the n local data from each country. We used these (① and ② in Fig. 2a) as benchmarks for our comparisons. We used the optimisation-based

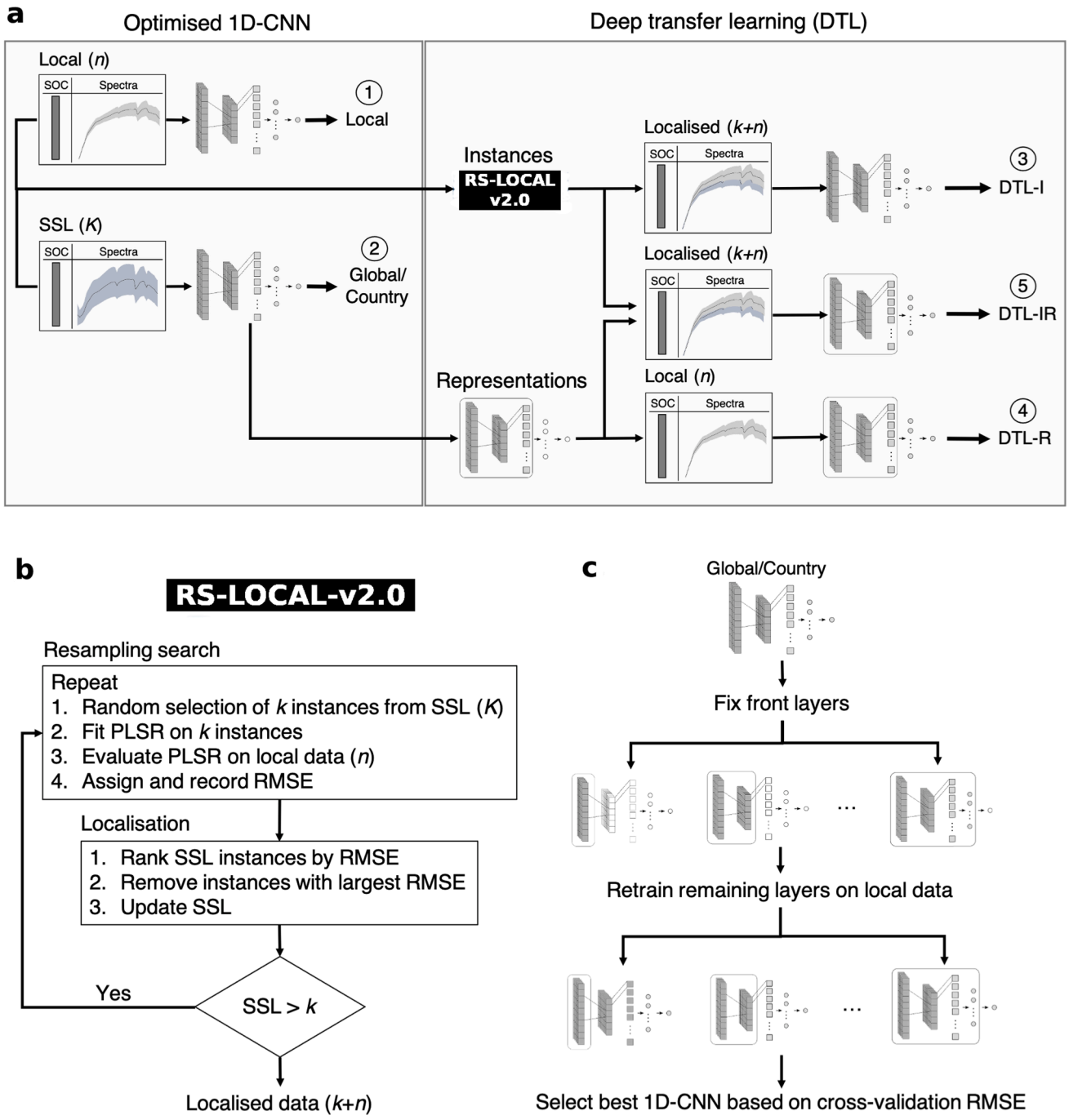

Fig. 2. Study design. (a) Flowchart for developing local, country, global and DTL 1D-CNNs. ① 1D-CNN developed on the n local data, ② 1D-CNN developed on the global/country SSL, ③ 1D-CNN developed on the $k+n$ localised data from the global or country SSL, ④ 1D-CNN transferred from global/country 1D-CNN to the local data, ⑤ 1D-CNN transferred from the global/country 1D-CNN to the localised data. (b) RS-LOCAL-v2.0 algorithm for transferring instances. (c) Transferring representations from a global/country 1D-CNN. Trained layers are in grey. Layers to be retrained are in white. Boxed layers are fixed during transfer.

framework for automated hyperparameter tuning described by Shen and Viscarra Rossel (2021) to train these 1D-CNNs. The framework stacks three types of building blocks: convolutional-blocks (Conv-blocks), fully-connected-blocks (FC-blocks) and an output-block to build a 1D-CNN. The number of the Conv- and FC-blocks and their internal hyperparameters are optimised to achieve an optimal architecture. In the Conv-blocks, the framework optimises hyperparameters: number of filters, kernel size, stride size in the convolutional layers, type and stride size in the pooling layers, activations functions, ON/OFF state of batch normalisation, pooling and dropout layers, and dropout rate. In the FC-blocks, it optimises the number of nodes in fully-connected layers, activation functions, ON/OFF state of the batch normalisation and dropout layers, and dropout rate. Other hyperparameters related to training: number of epochs, batch size, and optimisers, are also optimised. For a comprehensive list of hyperparameters optimised, please refer to the automated framework (Shen and Viscarra Rossel, 2021). The framework also incorporates different regularisation methods to prevent overfitting, such as batch normalisation (Ioffe and Szegedy, 2015), dropout (Srivastava et al., 2014), early-stopping (Prechelt, 1998), and cross-validation (Hutter et al., 2019), which allow 1D-CNN to perform well on small datasets. We used 10-fold cross-validation to develop the 1D-CNNs and root mean squared error (RMSE) to guide model selection. A SSL or dataset from a local site was randomly split into ten train-validation folds and a 1D-CNN was developed on each fold.

2.3.2. Transferring instances

We developed a new, improved version of the RS-LOCAL method (Lobsey et al., 2017), which we refer to as RS-LOCAL-V2.0 to transfer instances from the global and country SSLs to the local site-specific data from each country (Fig. 2b). RS-LOCAL-V2.0 is computationally more efficient, includes parallelisation and part of the algorithm is implemented in C++. Like the original algorithm described in Lobsey et al. (2017), RS-LOCAL-V2.0 is a data-mining search method that builds partial least square regression (PLSR) models recursively on subsets of an SSL, evaluates these models on a small number of labelled local data, n (in our case $n = 30$), and discards samples that consistently fall in poorly performing subsets until few useful samples for a given target and domain, k, are left. In our experiments $k = 100$. We found no significant advantage in selecting a larger subset. The selected k samples are then used to augment the n local data for modelling, hence the $k+n$ localised data.

2.3.3. Transferring representations

Global and country 1D-CNNs were developed, as described above, to learn representations from the SSLs. The representations were transferred from the global and country 1D-CNNs in a two-step manner (Fig. 2c). We first fixed the weights in the front layers and then retrained the remaining layers on the local/localised data with 10-fold cross-validation by randomly splitting the data into ten train-validation folds. The same ten folds were used in the 1D-CNNs when transferring representations from the global and country to the corresponding sites. Thus, representations learnt in the global and country 1D-CNN's front layers were used in the localised 1D-CNN. Depending on the number of front layers being fixed, there could be several localised 1D-CNNs for each local site. The one with the lowest cross-validation RMSE was considered the final model for transferring representations.

2.3.4. Deep transfer learning (DTL)

We transferred instances from the global and country SSLs as described above to generate the $k+n$ localised data and then developed optimal 1D-CNN to estimate SOC at the local sites from each country (DTL-I) (③ in Fig. 2a) using 10-fold cross-validation by randomly splitting the $k+n$ data into ten train-validation folds. When transferring representations from the global and country 1D-CNNs (described above), we evaluated the 1D-CNNs from the ten folds on the n local data and selected the fold with the smallest RMSE as the base model for the transfer because we assumed that it learnt the most useful representations for the particular local site. This significantly reduced the number of models to be transferred, by 90%, making the study computationally more feasible. We then transferred the representations of the base model to the n local data from each country (DTL-R) (④ in Fig. 2a) using the same ten folds as the local model. We also transferred instances and representations by combining the two approaches, that is, we transferred the representations from the global and country 1D-CNNs to the $k+n$ localised data from RS-LOCAL-V2.0 (DTL-IR) (⑤ in Fig. 2a) using the same ten folds as DTL-I.

In total, nine models were developed for the local site in each country. They are the local 1D-CNN with the n local data, the global 1D-CNN with the global SSL, country-specific 1D-CNN with the local site's corresponding country SSL, 1D-CNNs developed on the $k+n$ localised data from the global and country SSLs (DTL-I_g, DTL-I_c, respectively), 1D-CNNs developed by transferring representations from the global and country 1D-CNNs to the n local data (DTL-R_g, DTL-R_c, respectively), 1D-CNNs developed by transferring instances and representations from the global and country 1D-CNNs to the $k+n$ localised data (DTL-IR_g, DTL-IR_c, respectively).

2.4. Evaluation statistics

The final models were evaluated on the independently local test data ($N-n$, see above). We used the RMSEto measure inaccuracy, the mean error (ME) to assess bias, and the concordance correlation coefficient (ρ_c) (Lin, 1989) to enable comparisons between models and sites, with a single parameter that encompasses both bias and imprecision. ρ_c measures the difference between measured and estimated values and their deviation from a 45-degree line of perfect agreement. It ranges from −1 to 1, with 1 denoting perfect agreement.

For the different DTL approaches tested at each local site, we also assessed the change in RMSE compared to the local models by:

$$\Delta RMSE = (RMSE_{Local} - RMSE_{Other})/RMSE_{Local} \times 100 \quad (1)$$

where $RMSE_{Local}$ is the RMSE from local 1D-CNN. $RMSE_{Other}$ is the RMSE from the different DTL methods tested. ΔRMSE gives the RMSE change in percent units. A positive ΔRMSE means a better accuracy than the local 1D-CNN, while a negative ΔRMSE means a poorer accuracy.

3. Results

3.1. Transferring instances from SSLs using RS-LOCAL-V2.0

The statistical distributions of SOC (conditional distribution) in the global/country SSLs and the local data were markedly different (Table 1 and Fig. 3a). However, SOC distributions of the k data selected with RS-LOCAL-V2.0 were more similar to those of the local data (Fig. 3a). DTL-I from the SSLs using RS-LOCAL-V2.0 minimised the difference between the conditional distributions of the SSLs and n local data. Computation time for transferring instance using RS-LOCAL-V2.0 is proportional to the size of SSL. With the global SSL the transfer was completed in 7–8 min using Intel Xeon processors with 50 cores.

The first three PCs are shown in Fig. 3b. The larger variation of the global SSL compared to the country-specific SSLs highlights the greater diversity of soil data in the global library. The RS-LOCAL-V2.0 search selected data from similar and surrounding space to that occupied by the local data (Fig. 3b), thereby potentially aligning the marginal distributions of the global/country SSLs and the local data. Some local data from Sweden and the USA were outside of the PC space occupied by their respective countries SSLs, indicating that these country SSLs do not hold soils that represent all of those found in the local data. In contrast, by transferring instances from the global SSL with RS-LOCAL-V2.0, we could select data that closely represent the local data (Fig. 3b).

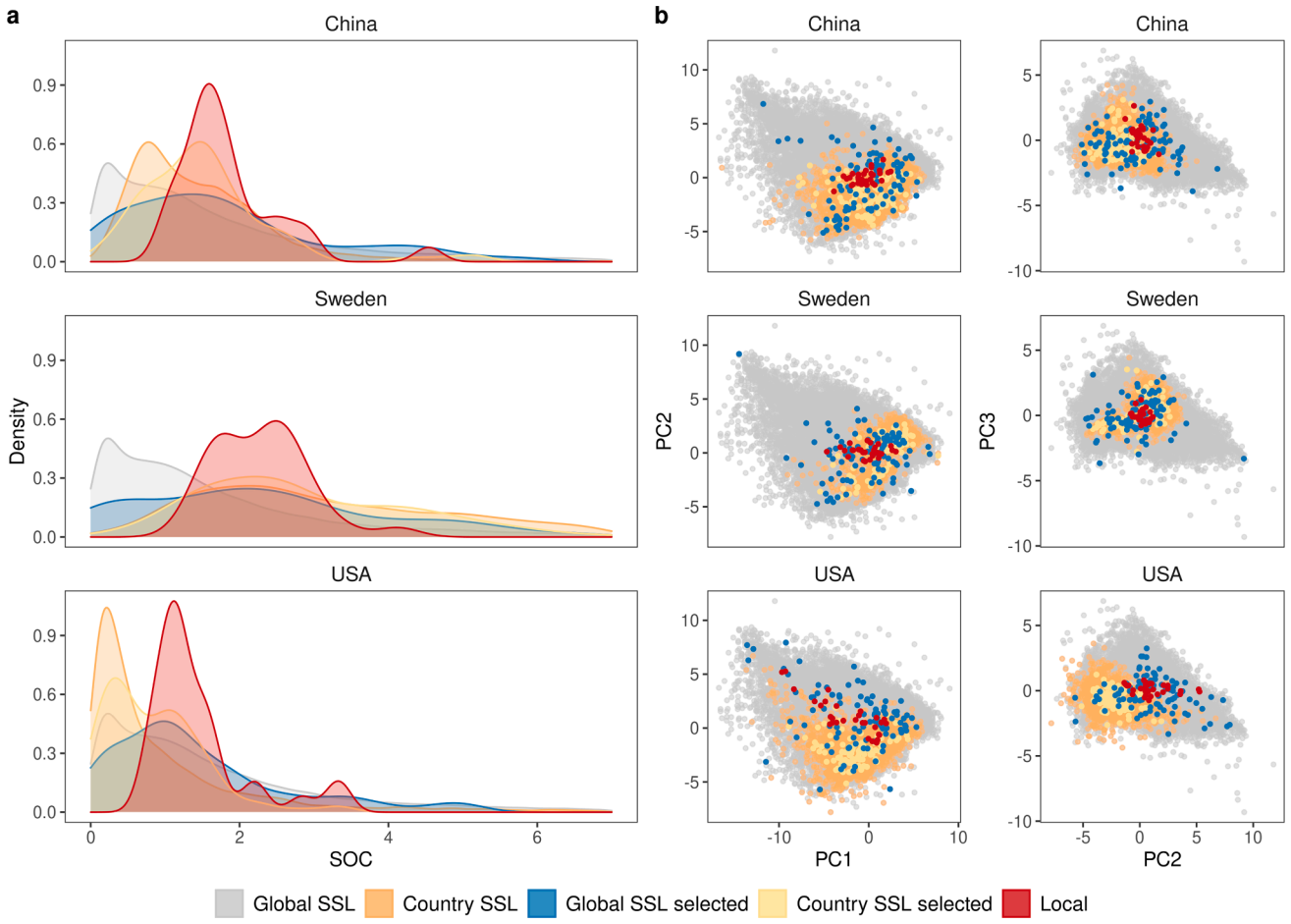

Fig. 3. Soil organic carbon (SOC %) distributions in the global/country SSLs, k RS-LOCAL-v2.0 selected data from the global/country SSLs and n local data, and principal component analysis on spectra from these datasets. (a) Density plot of SOC. (b) Principal components of the spectra from the different datasets.

3.2. Large-scale 1D-CNNs for transferring representations

The global and country-specific 1D-CNNs were optimised on the global and country-specific SSLs respectively. The models were developed in 2 to 22 days, depending on the size of the SSL and the specific implementation. Their architectures vary since they are data dependent (Fig. 2). The number of total blocks ranged from 4 (Sweden) to 8 (China), with different combinations of Conv- and FC-blocks. The architectural variations may indicate the different representations learnt in the 1D-CNNs. On the other hand, several hyperparameters in the architectures share similar values. For example, the 1D-CNNs tend to use large kernel sizes and large number of filters, and exclude pooling layers, which aligns with our previous findings on optimal 1D-CNNs for soil spectroscopic modelling (Shen and Viscarra Rossel, 2021). These 1D-CNNs served as the base models for transferring representations to the local sites (see Methods).

3.3. Comparing global, country, local and DTL models

We evaluated the global, country, local and DTL approaches by comparing the performance of their estimates of SOC on the $N-n$ independent test data from each of the local field and farm-scale sites (see Methods). The estimates of SOC in the farm and field sites with the global and country 1D-CNNs did not generalise well (Table 3), although for China, the model derived with its country SSL was better than the one derived with the global SSL. These estimates were generally the most biased (largest ME) and inaccurate (largest RMSE, smallest ρ_c) compared to the estimates with the local and DTL methods. The local 1D-CNNs and those derived with the different DTL methods produced estimates of SOC with similar accuracy (Table 3).

DTL $-I_g$ produced the most accurate estimates of SOC in all three examples. In the Chinese example RMSE $= 0.28\%$, $\rho_c = 0.84$, in the Swedish RMSE $= 0.23\%$, $\rho_c = 0.90$ and in the USA RMSE $= 0.31\%$, $\rho_c = 0.84$ (Table 3). The DTL-I_g estimates in the Swedish field were similar to the estimates made using the local data only (RMSE $= 0.24\%$, $\rho_c = 0.90$). In the USA field, estimates of SOC with DTL-I_g were almost identical to those from DTL-IR_g (RMSE $= 0.31\%$, $\rho_c = 0.85$) and estimates with the DTL-IR_c were also accurate (RMSE $= 0.32\%$, $\rho_c = 0.86$). Overall, DTL-I_g produced the smallest RMSE in all three local sites and largest ρ_c in all but the USA local site (Table 3).

To further quantitate the comparisons, we calculated the percent change in RMSE of the DTL estimates relative to local modelling (see Methods). Note we did not include the global or country 1D-CNNs because they were obviously biased (Table 3). Overall, compared to the local estimates, DTL-I_g improved the accuracy of the SOC estimates at the local sites by 25.8% on average (Fig. 4a). Fig. 4b shows plots of the observed versus the DTL-I_g estimates of SOC at each of the local sites. DTL-R_g and DTL-IR_g improved estimates of SOC only in the Chinese and USA local sites. DTL-I_c improved the local modelling of SOC in Chinese and USA local sites. DTL-R_c and DTL-IR_c did not show consistent improvements on the estimates from the purely local models. DTL-R_c only slightly improved the SOC estimates in the Chinese site, and DTL-IR_c improved the estimates in the USA site. In the Swedish local site, estimates of SOC with DTL-R_c and DTL-IR_c were inaccurate (Fig. 4a). Fig. 4c shows point maps of the estimated SOC values of all the N local data indicating the spatial variability of SOC in each site.

Table 2
Global and country 1D-CNN architectures. 1D-CNNs optimised on the global/country SSLs.

SSL	Block	Layers	Kernel/Pool size	Filters/Nodes	Padding type	Strides	Activation
Global	Conv-block	Convolutional	10 × 1	148	Valid	4 × 1	Swish
	–	Flatten	–	–	–	–	–
	FC-block 1	Fully-connected	–	691	–	–	SELU
	FC-block 2	Fully-connected	–	891	–	–	ELU
		Batch Normalisation	–	–	–	–	–
		Dropout (0.38)	–	–	–	–	–
	FC-block 3	Fully-connected	–	533	–	–	Swish
		Batch Normalisation	–	–	–	–	–
	FC-block 4	Fully-connected	–	764	–	–	SELU
		Batch normalisation	–	–	–	–	–
		Dropout (0.38)	–	–	–	–	–
	FC-block 5	Fully-connected	–	650	–	–	SELU
		Dropout (0.38)	–	–	–	–	–
	Output-block	Fully-connected	–	1	–	–	Linear
China	Conv-block 1	Convolutional	7 × 1	25	Valid	7 × 1	Swish
	Conv-block 2	Convolutional	8 × 1	248	Valid	3 × 1	LeakyReLU
	Conv-block 3	Convolutional	5 × 1	238	Valid	4 × 1	ReLU
		Dropout (0.39)	–	–	–	–	–
	–	Flatten	–	–	–	–	–
	FC-block 1	Fully-connected	–	212	–	–	LeakyReLU
		Dropout (0.07)	–	–	–	–	–
	FC-block 2	Fully-connected	–	140	–	–	LeakyReLU
	FC-block 3	Fully-connected	–	165	–	–	Swish
	FC-block 4	Fully-connected	–	50	–	–	LeakyReLU
		Dropout (0.07)	–	–	–	–	–
	Output-block	Fully-connected	–	1	–	–	Linear
Sweden	Conv-block	Convolutional	5 × 1	161	Valid	3 × 1	ELU
	–	Flatten	–	–	–	–	–
	FC-block 1	Fully-connected	–	896	–	–	Swish
		Batch normalisation	–	–	–	–	–
		Dropout (0.37)	–	–	–	–	–
	FC-block 2	Fully-connected	–	474	–	–	Swish
		Batch normalisation	–	–	–	–	–
		Dropout (0.37)	–	–	–	–	–
	Output-block	Fully-connected	–	1	–	–	Linear
USA	Conv-block 1	Convolutional	8 × 1	216	Valid	7 × 1	SELU
	Conv-block 2	Convolutional	8 × 1	216	Same	8 × 1	Swish
		Batch normalisation	–	–	–	–	–
	Conv-block 3	Convolutional	4 × 1	252	Same	4 × 1	LeakyReLU
		Dropout (0.03)	–	–	–	–	–
	–	Flatten	–	–	–	–	–
	FC-block 1	Fully-connected	–	179	–	–	Swish
		Batch normalisation	–	–	–	–	–
	FC-block 2	Fully-connected	–	252	–	–	Swish
		Batch normalisation	–	–	–	–	–
		Dropout (0.29)	–	–	–	–	–
	Output-block	Fully-connected	–	1	–	–	Linear

3.4. 1D-CNN architectures of DTL-I_g

Given that DTL-I_g produced the most accurate local estimates of SOC at each site, we show their 1D-CNN architectures in Table 4. Only a few Conv-blocks were used in the architectures, and they tended to use large kernel size and number of filters in the convolutional layers. The architectures had one Conv-block and up to two FC-blocks. Pooling layers were disabled in the all the Conv-blocks. Again, these architectures aligned well with our previous findings on optimal 1D-CNNs for soil spectroscopic modelling (Shen and Viscarra Rossel, 2021).

4. Discussion

There is global interest in soil spectroscopy because one can use spectra to estimate, with various degrees of success, soil chemical, physical and biological properties (Song et al., 2021; Soriano-Disla et al., 2014; Yang et al., 2019, 2022). To do so, however, we need to develop an SSL, and there's been significant investment in developing large and diverse SSLs (e.g. Viscarra Rossel and Webster, 2012; Shi et al., 2014; Wijewardane et al., 2016; Gogé et al., 2012; Dematte et al., 2019; Peng et al., 2013; Orgiazzi et al., 2018; Viscarra Rossel et al., 2016; Brown et al., 2006; Stevens et al., 2013). Recently, much of the interest in soil spectroscopy has been for the estimation of SOC. The reason is that soil spectroscopy is cost-efficient (Li et al., 2022) and conventional methods for measuring and monitoring SOC content are time-consuming, expensive and present a key barrier to the design and implementation of practices that could increase SOC and their MRV (England and Viscarra Rossel, 2018; Paustian et al., 2019). The spectroscopic method can be extended to the estimation of SOC with hyperspectral remote sensing (Castaldi et al., 2019), which can be used to complement on-ground spectroscopic estimates to cover much larger areas. If we could increase the content of SOC, it could help to mitigate climate change, improve soil health, ecosystem resilience, and food security (Smith et al., 2020).

A large SSL that captures soil variation globally is complex and rich in information. Therefore, modelling of soil properties using SSLs for accurate estimation at a local site is challenging. Here, we developed a robust DTL method to accurately transfer the valuable information in large and diverse SSLs to enable rapid, cost-effective and accurate local estimates of SOC at the farm or field scale. Our results show that DTL-I effectively leverages helpful information from the large, global SSL to lessen the need for conventional laboratory analysis of soil samples,

Table 3
Test statistics of soil organic carbon (SOC %) predictions at the local sites. Subscripts of the DTL methods indicate the SSL used: *g* for the global SSL and *c* for country SSLs.

Statistics	Modelling		China	Sweden	USA
	SSL	1D-CNN			
RMSE	–	Local	0.46	0.24	0.47
	Global	Global	0.77	1.06	1.02
		DTL-I_g	0.28	0.23	0.31
		DTL-R_g	0.45	0.28	0.35
		DTL-IR_g	0.31	0.33	0.31
	Country	Country	0.51	1.10	2.89
		DTL-I_c	0.36	0.39	0.33
		DTL-R_c	0.42	1.10	0.55
		DTL-IR_c	0.45	0.86	0.32
ME	–	Local	−0.02	−0.05	−0.07
	Global	Global	−0.15	−0.95	0.44
		DTL-I_g	−0.11	0.04	−0.09
		DTL-R_g	0.05	−0.01	−0.05
		DTL-IR_g	0.01	−0.14	−0.09
	Country	Country	−0.21	−0.56	1.98
		DTL-I_c	0.09	−0.29	0.05
		DTL-R_c	0.11	0.18	0.17
		DTL-IR_c	0.11	−0.59	−0.01
ρ_c	–	Local	0.59	0.90	0.70
	Global	Global	0.54	0.33	0.46
		DTL-I_g	0.84	0.90	0.84
		DTL-R_g	0.42	0.81	0.80
		DTL-IR_g	0.80	0.82	0.85
	Country	Country	0.62	−0.30	0.23
		DTL-I_c	0.72	0.73	0.82
		DTL-R_c	0.52	−0.54	0.75
		DTL-IR_c	0.48	0.05	0.86

thereby reducing the time required for measuring and improving the cost-effectiveness of SOC assessments. Thus, one can process many more soil samples for a little additional cost and better characterise soil spatial and temporal variability to support SOC MRV (FAO, 2020).

Modelling SOC (and more generally, soil properties) directly with large SSLs (e.g. global or country) does not work well when the 'global' models are used to estimate locally, e.g. the SOC in an agricultural field. Typically, the estimates produced are biased. This has led researchers and practitioners to question the need and usefulness of large spectral libraries (Guerrero et al., 2016). However, our results show that large SSLs with vast and diverse soils are useful for DTL because they can supply information to localise the models and improve the accuracy of SOC estimates at a site. In this regard, the more extensive and diverse global SSL was more effective for DTL than the smaller country SSLs.

The modelling problem lies in the dissimilarity of the conditional and marginal distributions between the training data from the large SSLs, and the 'unknown' local data (Pan and Yang, 2009; Weiss et al., 2016). That is, when the statistical distributions of the response and predictor variables between the training and local data are too different, the model derived with the large SSL cannot depict the variability in the local data, and its generalisation capacity diminishes. Here, we have shown that DTL-I can help to reduce the differences between these distributions (Fig. 3). Transferring instances with RS-LOCAL-v2.0 discarded 99 % of the instances in the global SSL, keeping only the most useful ones for the local modelling. The search, filtering and localisation that the algorithm performs help with the marginal and conditional distributions. As a result, DTL-I with the global SSL produced the most accurate estimates of SOC at each of the local sites in each country. DTL-I with 1D-CNN can also handle data with different complexity. When a dataset is small, relatively homogeneous and with linear response, modelling with a linear method such as PLSR will be appropriate. However, if the dataset is small but heterogeneous and with non-linear response, then PLSR will not be sufficient for modelling, thereby needing more complex (non-linear) methods like machine learning and 1D-CNNs. In real-world situations, it is difficult to determine which algorithm to use, making 1D-CNN a sensible choice as it is able to handle data with different levels of complexity to generate reliable predictions. Because we incorporated different regularisation methods in the optimisation framework (Shen and Viscarra Rossel, 2021), the risk of overfitting 1D-CNN on the $k+n$ localised data is also minimised.

Deep transfer learning of instances from a global SSL requires extracting instances from the SSL using RS-LOCAL-v2.0 and deriving an optimal 1D-CNN using the automated framework (Shen and Viscarra Rossel, 2021). The RS-LOCAL-v2.0 selection finished within several minutes using 50 CPU cores. However, evaluating hundreds 1D-CNNs in sequence to find a best one could take 20 h on a single GPU. Future improvements will explore other hyperparameter optimisation algorithms (Li et al., 2017; Jamieson and Talwalkar, 2016) to parallelise the evaluations, which would greatly improve the computation efficiency of DTL-I_g, and the use of other machine learning methods.

The few examples in the literature of DTL for spectroscopic modelling of SOC have focused on DTL-R using continental SSLs and transferring to country or regional levels (Liu et al., 2018; Padarian et al., 2019). Here, we found DTL-R generally inconsistent for transferring information from the larger SSLs to estimate SOC in a farm or field. DTL-R using the global data was only useful for estimating SOC in the USA local site. There are several reasons for this. A large SSL contains inconsistencies arising from various sources, e.g. different analytical methods, calibration protocols and standards, and insufficient sampling, etc. Such inconsistencies can affect the quality of the representations learnt in the large-scale 1D-CNNs. Inconsistencies may also exist between the local data and SSL, thus the learnt representations may not apply to some local sites. This is also the reason why localisation based on spectral similarity using distance metrics perform inconsistently. It could also be that soil vis–NIR spectra are largely non-specific, and the learned features in the 1D-CNNs are data dependent, limiting the generalisation of the representations. Moreover, the networks may rote learn all of the information (cf. Webster et al., 2021) and the 1D-CNNs derived with the global and country SSLs can contain both helpful and irrelevant representations for the SOC estimates at a site. These may explain the varied performance of DTL-R and DTL-IR (Fig. 4a), and the relatively minor improvements in the estimates reported elsewhere (Liu et al., 2018; Padarian et al., 2019). Although our results show that DTL-I to be generally better than DTL-IR, there is value in transferring both, instances and representations (Fig. 4). If we could exclude the irrelevant learned features for the transfer, via robust feature selection for example, the performance of DTL-R and DTL-IR should improve.

Errors and other disturbances exist in any SSL when the spectra are measured with different instrument and under different conditions, resulting in additive or multiplicative errors, random noise, or shifting wavelengths. The SOC analysed in laboratories can also suffer from errors that may be due to the different methods used, or the different protocols in different laboratories. DTL can attenuate such disturbances. The unique architecture of CNN enables local transnational invariance (LeCun et al., 2015), which can handle errors in the measurements of spectra, such as shifting wavelengths, and DTL-I can filter the errors and disturbances in the spectra and in the SOC data, keeping only the most relevant data for the modelling. Thus, DTL should remove the need for conventional calibration transfer, which requires a 'master' instrument and additional resources for making the empirical corrections (Workman, 2018).

5. Conclusions

Using large SSLs to accurately estimate SOC locally is challenging and the focus of research over the past decades. We employed DTL to solve this problem via transferring instances from large-scale SSLs, transferring representations from 1D-CNN trained on the SSLs, and transferring both instances and representations to assist local modelling. Transferring instances effectively used information from the global SSL

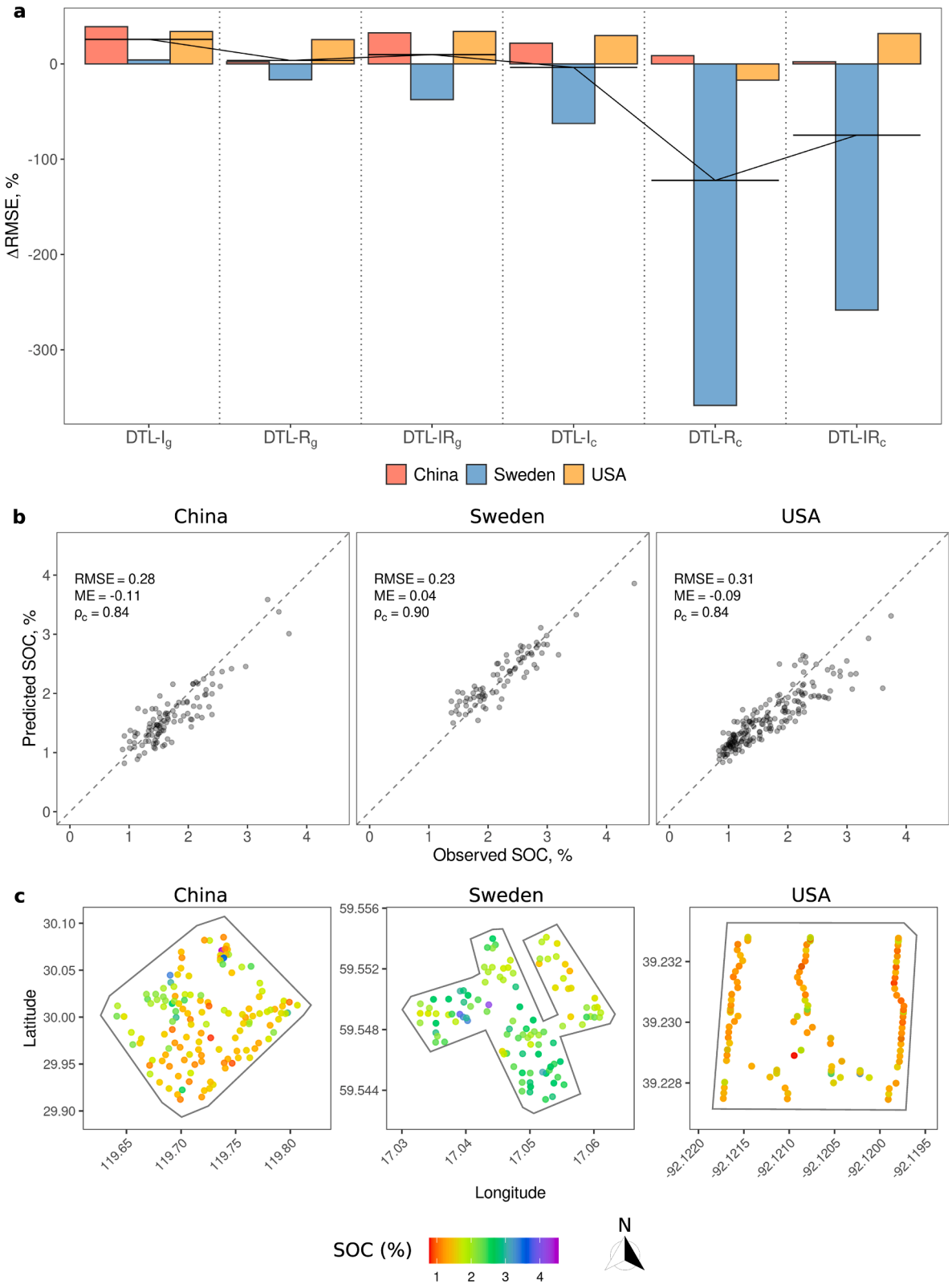

Fig. 4. Comparing estimates of SOC with DTL and local models. (a) Percent reduction in RMSE from DTL compared to local modelling. A positive ΔRMSE suggests that the DTL method produced more accurate estimates of SOC compared to the local model, while a negative ΔRMSE indicates that the DTL estimates were less accurate than those from the local model. The solid line gives the mean ΔRMSE of the three sites for each method. (b) Plots of estimated versus observed SOC at the local sites from DTL-I_g, which was the best method. (c) Spatial point distribution of the estimates of SOC at each site.

Table 4
DTL-I_g 1D-CNN architectures. Optimal 1D-CNNs developed on the localised data from the global SSL (③ in Fig. 2a).

Local site	Block	Layer	Kernel/Pool size	Filters/Nodes	Padding	Strides	Activation
China	Conv-block	Convolutional	3 × 1	232	Valid	2 × 1	Swish
		Dropout (0.001)	–	–	–	–	–
	–	Flatten	–	–	–	–	–
	FC-block	Fully-connected	–	22	–	–	ELU
		Dropout (0.38)	–	–	–	–	–
	Output-block	Fully-connected	–	1	–	–	Linear
Sweden	Conv-block	Convolutional	10 × 1	214	Same	6 × 1	SELU
		Dropout (0.20)	–	–	–	–	–
	–	Flatten	–	–	–	–	–
	FC-block 1	Fully-connected	–	446	–	–	LeakyReLU
		Batch Normalisation	–	–	–	–	–
	FC-block 2	Fully-connected	–	208	–	–	Swish
		Dropout (0.48)	–	–	–	–	–
	Output-block	Fully-connected	–	1	–	–	Linear
USA	Conv-block	Convolutional	7 × 1	212	Same	3 × 1	Swish
		Dropout (0.16)	–	–	–	–	–
	–	Flatten	–	–	–	–	–
	FC-block 1	Fully-connected	–	1005	–	–	Swish
	FC-block 2	Fully-connected	–	1015	–	–	SELU
	Output-block	Fully-connected	–	1	–	–	Linear

to most accurately estimate SOC in each local site, reducing RMSE by 25.8% on average.

We showed that large SSLs contain helpful information that can be transferred locally with DTL to improve the modelling and estimation of SOC. Thus, our study confirms that there is value in developing and maintaining large SSLs and highlights the need to expand SSLs to encompass the vast diversity of global soils to solve real-world problems. In this case, the methods presented here could help estimate SOC anywhere in the world more accurately, rapidly, and cost-effectively, enabling MRV protocols to monitor SOC changes.

Author contributions

RAVR conceived the research and designed the study and methods with ZS, LR-L, TB and LC. ZS carried out the experiments and with RAVR, LR-L and TB drafted the manuscript., MZ, LW, JW, ZS, KS, PB, YS, KC contributed to the experimental design, data from the local sites and helped to improve the manuscript. All authors discussed and interpreted the results and produced the final manuscript.

Declaration of Competing Interest

The authors declare that they have no known competing financial interests or personal relationships that could have appeared to influence the work reported in this paper.

Acknowledgements

This work was funded by the Research office at Curtin University and was supported by the Pawsey Supercomputing Centre with funding from the Australian Government and the Government of Western Australia. We thank the providers of the various spectral libraries used in this work (ISRIC, LUCAS, USA, Mediterranean, Chinese) as well as the voluntary global spectral library project and the many people that contributed to the global spectral library, listed in Viscarra Rossel et al. (2016).

References

Barnes, R.J., Dhanoa, M.S., Lister, S.J., 1989. Standard normal variate transformation and de-trending of near-infrared diffuse reflectance spectra. Appl. Spectrosc. 43 (5), 772–777. https://doi.org/10.1366/0003702894202201.

Brown, D.J., 2007. Using a global vnir soil-spectral library for local soil characterization and landscape modeling in a 2nd-order uganda watershed. Geoderma 140 (4), 444–453.

Brown, D.J., Shepherd, K.D., Walsh, M.G., Mays, M.D., Reinsch, T.G., 2006. Global soil characterization with VNIR diffuse reflectance spectroscopy. Geoderma 132 (3–4), 273–290. https://doi.org/10.1016/j.geoderma.2005.04.025.

Castaldi, F., Hueni, A., Chabrillat, S., Ward, K., Buttafuoco, G., Bomans, B., Vreys, K., Brell, M., van Wesemael, B., 2019. Evaluating the capability of the sentinel 2 data for soil organic carbon prediction in croplands. ISPRS J. Photogramm. Remote Sens. 147, 267–282. https://doi.org/10.1016/j.isprsjprs.2018.11.026.

Clairotte, M., Grinand, C., Kouakoua, E., Thébault, A., Saby, N.P., Bernoux, M., Barthès, B.G., 2016. National calibration of soil organic carbon concentration using diffuse infrared reflectance spectroscopy. Geoderma 276, 41–52.

Cui, Y., Song, Y., Sun, C., Howard, A., Belongie, S., 2018. Large scale fine-grained categorization and domain-specific transfer learning, in. In: Proceedings of the IEEE conference on computer vision and pattern recognition, pp. 4109–4118.

Demattê, J.A., Dotto, A.C., Paiva, A.F., Sato, M.V., Dalmolin, R.S., Maria do Socorro, B., da Silva, E.B., Nanni, M.R., ten Caten, A., Noronha, N.C., et al., 2019. The brazilian soil spectral library (bssl): A general view, application and challenges. Geoderma 354, 113793.

England, J.R., Viscarra Rossel, R.A., 2018. Proximal sensing for soil carbon accounting. Soil 4 (2), 101–122. https://doi.org/10.5194/soil-4-101-2018.

FAO, 2020. A protocol for measurement, monitoring, reporting and verification of soil organic carbon in agricultural landscapes: GSOC MRV protocol. FAO, Rome, Italy.

Field, C.B., Raupach, M.R., 2004. The global carbon cycle: integrating humans, climate, and the natural world, vol. 62. Island Press.

Food, A.O. (FAO), 1998. Soils map of the world: revised legend. Tech. rep. Food and Agriculture Organization of the United Nations.

Gao, Y., Cui, Y., 2020. Deep transfer learning for reducing health care disparities arising from biomedical data inequality. Nat. Commun. 11 (1), 1–8.

Gogé, F., Joffre, R., Jolivet, C., Ross, I., Ranjard, L., 2012. Optimization criteria in sample selection step of local regression for quantitative analysis of large soil nirs database. Chemometr. Intell. Lab. Syst. 110 (1), 168–176.

Gogé, F., Gomez, C., Jolivet, C., Joffre, R., 2014. Which strategy is best to predict soil properties of a local site from a national vis–nir database? Geoderma 213, 1–9.

Guerrero, C., Stenberg, B., Wetterlind, J., Viscarra Rossel, R.A., Maestre, F.T., Mouazen, A.M., Zornoza, R., Ruiz-Sinoga, J.D., Kuang, B., 2014. Assessment of soil organic carbon at local scale with spiked NIR calibrations: effects of selection and extra-weighting on the spiking subset. European Journal of Soil Science 65, 248–263.

Guerrero, C., Wetterlind, J., Stenberg, B., Mouazen, A.M., Gabarrón-Galeote, M.A., Ruiz-Sinoga, J.D., Zornoza, R., Viscarra Rossel, R.A., 2016. Do we really need large spectral libraries for local scale soc assessment with nir spectroscopy? Soil Tillage Res. 155, 501–509.

Guo, Y., Shi, H., Kumar, A., Grauman, K., Rosing, T., Feris, R., 2019. Spottune: transfer learning through adaptive fine-tuning, in. In: Proceedings of the IEEE/CVF conference on computer vision and pattern recognition, pp. 4805–4814.

Hutter, F., Kotthoff, L., Vanschoren, J., 2019. Automated machine learning: methods, systems, challenges. Springer Nature.

i BEC, TAU, USCM, UZAY, FASF, IPB, SRTI, CUT, CEDARE, The regional soil spectral library, 2019. http://datahub.geocradle.eu/dataset/regional-soil-spectral-library.

W.A. (ICRAF), I.S. Reference, I.C. (ISRIC), ICRAF-ISRIC Soil VNIR Spectral Library, 2021. doi:10.34725/DVN/MFHA9C. https://doi.org/10.34725/DVN/MFHA9C.

Ioffe, S., Szegedy, C., 2015. Batch normalization: Accelerating deep network training by reducing internal covariate shift. In: International conference on machine learning, PMLR, pp. 448–456.

Jamieson, K., Talwalkar, A., 2016. Non-stochastic best arm identification and hyperparameter optimization. In: Artificial Intelligence and Statistics. PMLR, pp. 240–248.

Kang, Y., Cho, N., Yoon, J., Park, S., Kim, J., 2021. Transfer learning of a deep learning model for exploring tourists' urban image using geotagged photos. ISPRS Int. J. Geo-Inform. 10 (3), 137.
Kennard, R.W., Stone, L.A., 1969. Computer aided design of experiments. Technometrics 11 (1), 137–148.
Lal, R., 2004. Soil carbon sequestration impacts on global climate change and food security. Science 304 (5677), 1623–1627.
LeCun, Y., Bengio, Y., Hinton, G., 2015. Deep learning. Nature 521 (7553), 436–444.
Lehmann, J., Kleber, M., 2015. The contentious nature of soil organic matter. Nature 528 (7580), 60–68.
Li, L., Jamieson, K., DeSalvo, G., Rostamizadeh, A., Talwalkar, A., 2017. Hyperband: A novel bandit-based approach to hyperparameter optimization. J. Mach. Learn. Res. 18 (1), 6765–6816.
Li, H., Li, Y., Yang, M., Chen, S., Zhou, S., 2021. Strategy of efficient estimation of soil organic content at the local scale based on the national spectral database. Authorea Preprints. https://doi.org/10.22541/AU.163283455.51380609/V1.
Li, S., Viscarra Rossel, R.A., Webster, R., 2022. The cost-effectiveness of reflectance spectroscopy for estimating soil organic carbon. Eur. J. Soil Sci. 73 (1), e13202. https://doi.org/10.1111/ejss.13202.
Lin, L.I.-K., 1989. A concordance correlation coefficient to evaluate reproducibility. Biometrics 255–268.
Liu, L., Ji, M., Buchroithner, M., 2018. Transfer learning for soil spectroscopy based on convolutional neural networks and its application in soil clay content mapping using hyperspectral imagery. Sensors 18 (9), 3169.
Lobsey, C., Viscarra Rossel, R.A., Roudier, P., Hedley, C., 2017. rs-local data-mines information from spectral libraries to improve local calibrations. Eur. J. Soil Sci. 68 (6), 840–852.
Mateo-García, G., Laparra, V., López-Puigdollers, D., Gómez-Chova, L., 2020. Transferring deep learning models for cloud detection between landsat-8 and proba-v. ISPRS J. Photogramm. Remote Sens. 160, 1–17.
Naes, T., Isaksson, T., Kowalski, B., 1990. Locally weighted regression and scatter correction for near-infrared reflectance data. Anal. Chem. 62 (7), 664–673.
Orgiazzi, A., Ballabio, C., Panagos, P., Jones, A., Fernández-Ugalde, O., 2018. Lucas soil, the largest expandable soil dataset for europe: a review. Eur. J. Soil Sci. 69 (1), 140–153.
Padarian, J., Minasny, B., McBratney, A., 2019. Transfer learning to localise a continental soil vis-nir calibration model. Geoderma 340, 279–288.
Pan, S.J., Yang, Q., 2009. A survey on transfer learning. IEEE Trans. Knowl. Data Eng. 22 (10), 1345–1359.
Paustian, K., Collier, S., Baldock, J., Burgess, R., Creque, J., DeLonge, M., Dungait, J., Ellert, B., Frank, S., Goddard, T., Govaerts, B., Grundy, M., Henning, M., Izaurralde, R.C., Madaras, M., McConkey, B., Porzig, E., Rice, C., Searle, R., Seavy, N., Skalsky, R., Mulhern, W., Jahn, M., 2019. Quantifying carbon for agricultural soil management: from the current status toward a global soil information system. Carbon Manage. 10 (6), 567–587. https://doi.org/10.1080/17583004.2019.1633231.
Peng, Y., Knadel, M., Gislum, R., Deng, F., Norgaard, T., de Jonge, L.W., Moldrup, P., Greve, M.H., 2013. Predicting soil organic carbon at field scale using a national soil spectral library. J. Near Infrared Spectrosc. 21 (3), 213–222.
Prechelt, L., 1998. Early stopping-but when?. In: Neural Networks: Tricks of the trade. Springer, pp. 55–69.
Ramirez-Lopez, L., Behrens, T., Schmidt, K., Stevens, A., Demattê, J.A.M., Scholten, T., 2013. The spectrum-based learner: A new local approach for modeling soil vis–nir spectra of complex datasets. Geoderma 195, 268–279.
Sankey, J.B., Brown, D.J., Bernard, M.L., Lawrence, R.L., 2008. Comparing local vs. global visible and near-infrared (visnir) diffuse reflectance spectroscopy (drs) calibrations for the prediction of soil clay, organic c and inorganic c. Geoderma 148 (2), 149–158.
Schlesinger, W.H., 1977. Carbon balance in terrestrial detritus. Ann. Rev. Ecol. Systematics 8 (1), 51–81.
Seidel, M., Hutengs, C., Ludwig, B., Thiele-Bruhn, S., Vohland, M., 2019. Strategies for the efficient estimation of soil organic carbon at the field scale with vis–NIR spectroscopy: Spectral libraries and spiking vs. local calibrations. Geoderma 354, 113856. https://doi.org/10.1016/J.Geoderma.2019.07.014.
Shen, Z., Viscarra Rossel, R.A., 2021. Automated spectroscopic modelling with optimised convolutional neural networks. Sci. Rep. 11 (1), 1–12.
Shenk, J.S., Westerhaus, M.O., Berzaghi, P., 1997. Investigation of a local calibration procedure for near infrared instruments. J. Near Infrared Spectrosc. 5 (4), 223–232.
Shepherd, K.D., Palm, C.A., Gachengo, C.N., Vanlauwe, B., 2003. Rapid characterization of organic resource quality for soil and livestock management in tropical agroecosystems using near-infrared spectroscopy. Agron. J. 95 (5), 1314–1322. https://doi.org/10.2134/agronj2003.1314.
Shi, Z., Wang, Q., Peng, J., Ji, W., Liu, H., Li, X., Viscarra Rossel, R.A., 2014. Development of a national vnir soil-spectral library for soil classification and prediction of organic matter concentrations. Sci. China Earth Sci. 57, 167–1680. https://doi.org/10.1007/s11430-013-4808-x.
Shi, Z., Ji, W., Viscarra Rossel, R.A., Chen, S., Zhou, Y., 2015. Prediction of soil organic matter using a spatially constrained local partial least squares regression and the chinese vis–nir spectral library. Eur. J. Soil Sci. 66 (4), 679–687.
Smith, P., Soussana, J., Angers, D., Schipper, L., Chenu, C., Rasse, D.P., Batjes, N.H., Egmond, F., McNeill, S., Kuhnert, M., Arias-Navarro, C., Olesen, J.E., Chirinda, N., Fornara, D., Wollenberg, E., Álvaro-Fuentes, J., Sanz-Cobena, A., Klumpp, K., 2020. How to measure, report and verify soil carbon change to realize the potential of soil carbon sequestration for atmospheric greenhouse gas removal. Glob. Change Biol. 26 (1), 219–241. https://doi.org/10.1111/gcb.14815.
Song, Yongze, Shen, Zefang, Wu, Peng, Viscarra Rossel, R.A., 2021. Wavelet geographically weighted regression for spectroscopic modelling of soil properties. Scientific Reports 11, 1–11, 1.
Soriano-Disla, J.M., Janik, L.J., Viscarra Rossel, R.A., Macdonald, L.M., McLaughlin, M. J., 2014. The Performance of Visible, Near-, and Mid-Infrared Reflectance Spectroscopy for Prediction of Soil Physical, Chemical, and Biological Properties. Appl. Spectrosc. Rev. 49 (2), 139–186. https://doi.org/10.1080/05704928.2013.811081.
Srivastava, N., Hinton, G., Krizhevsky, A., Sutskever, I., Salakhutdinov, R., 2014. Dropout: a simple way to prevent neural networks from overfitting. J. Mach. Learn. Res. 15 (1), 1929–1958.
Stenberg, B., Viscarra Rossel, R.A., Mouazen, A.M., Wetterlind, J., 2010. Visible and near infrared spectroscopy in soil science. Adv. Agron. 107, 163–215.
Stevens, A., Ramirez-Lopez, L., 2014. An introduction to the prospectr package, R Package Vignette, Report No.: R Package Version 0.1 3.
Stevens, A., Nocita, M., Tóth, G., Montanarella, L., van Wesemael, B., 2013. Prediction of soil organic carbon at the european scale by visible and near infrared reflectance spectroscopy. PloS One 8 (6), e66409. https://doi.org/10.1371/journal.pone.0066409.
Tan, C., Sun, F., Kong, T., Zhang, W., Yang, C., Liu, C., 2018. A survey on deep transfer learning. In: International conference on artificial neural networks. Springer, pp. 270–279.
Tsakiridis, N.L., Theocharis, J.B., Symeonidis, A.L., Zalidis, G.C., 2021. Improving the predictions of soil properties from VNIR-SWIR spectra in an unlabeled region using semi-supervised and active learning. Geoderma 387, 114830. https://doi.org/10.1016/J.Geoderma.2020.114830.
Viscarra Rossel, R.A., Webster, R., 2012. Predicting soil properties from the australian soil visible–near infrared spectroscopic database. Eur. J. Soil Sci. 63 (6), 848–860.
Viscarra Rossel, R.A., Cattle, S.R., Ortega, A., Fouad, Y., 2009. In situ measurements of soil colour, mineral composition and clay content by vis–nir spectroscopy. Geoderma 150 (3–4), 253–266.
Viscarra Rossel, R.A., Behrens, T., Ben-Dor, E., Brown, D., Demattê, J., Shepherd, K.D., Shi, Z., Stenberg, B., Stevens, A., Adamchuk, V., et al., 2016. A global spectral library to characterize the world's soil. Earth Sci. Rev. 155, 198–230.
Webster, R., Rabin, J., Simon, L., Jurie, F., 2021. This person (probably) exists. identity membership attacks against gan generated faces, arXiv preprint arXiv:2107.06018.
Weiss, K., Khoshgoftaar, T.M., Wang, D., 2016. A survey of transfer learning. J. Big Data 3 (1), 1–40.
Wetterlind, J., Stenberg, B., 2010. Near-infrared spectroscopy for within-field soil characterization: small local calibrations compared with national libraries spiked with local samples. Eur. J. Soil Sci. 61 (6), 823–843.
Wijewardane, N.K., Ge, Y., Wills, S., Loecke, T., 2016. Prediction of soil carbon in the conterminous united states: Visible and near infrared reflectance spectroscopy analysis of the rapid carbon assessment project. Soil Sci. Soc. Am. J. 80 (4), 973–982.
Wold, S., Esbensen, K., Geladi, P., 1987. Principal component analysis. Chemometr. Intell. Lab. Syst. 2 (1–3), 37–52.
Workman, J.J., 2018. A review of calibration transfer practices and instrument differences in spectroscopy. Appl. Spectrosc. 72 (3), 340–365.
Wurm, M., Stark, T., Zhu, X.X., Weigand, M., Taubenböck, H., 2019. Semantic segmentation of slums in satellite images using transfer learning on fully convolutional neural networks. ISPRS J. Photogramm. Remote Sens. 150, 59–69.
Yang, Y., Viscarra Rossel, R.A., Li, S., Bissett, A., Lee, J., Shi, Z., Behrens, T., Court, L., 2019. Soil bacterial abundance and diversity better explained and predicted with spectro-transfer functions. Soil Biol. Biochem. 129, 29–38. https://doi.org/10.1016/j.soilbio.2018.11.005.
Yang, Y., Shen, Z., Bissett, A., Viscarra Rossel, R.A., 2022. Estimating soil fungal abundance and diversity at a macroecological scale with deep learning spectrotransfer functions. Soil 8 (1), 223–235. https://doi.org/10.5194/soil-8-223-2022.
Zoph, B., Yuret, D., May, J., Knight, K., 2016. Transfer learning for low-resource neural machine translation, arXiv preprint arXiv:1604.02201.